South Tethyan passive margin paleoslope orientation inferred from soft-sediment deformation and fault kinematic analysis: a case study from the Cretaceous of Borj Cedria area, Tunisia

Chahreddine Naji, Zayneb Amri, Amara Masrouhi, Olivier Bellier

South Tethyan passive margin paleoslope orientation inferred from soft-sediment deformation and fault kinematic analysis: a case study from the Cretaceous of Borj Cedria area, Tunisia

Chahreddine Naji [a]*, Zayneb Amri [a], Amara Masrouhi [a, b], Olivier Bellier [c]

[a] Geo-Resources Laboratory, Water Research and Technologies Center Borj-Cedria, & Carthage University, Faculty of Sciences of Bizerte, Tunisia.

[b] King Abdulaziz University, Faculty of Earth Sciences, Department of Structural Geology and Remote Sensing, Jeddah, Saudi Arabia.

[c] Aix Marseille Univ, CNRS, IRD, INRAE, Coll France, CEREGE, Aix-en-Provence, France.

* Corresponding author: chahreddine.naji.geo@gmail.com

Abstract

The Cretaceous outcrops of Borj Cedria-Bou Kournine area belongs to the NE-trending Atlas system of northern Tunisia. This area exposes sub-meridian folds associated with numerous N- to NW-trending major fault systems. This study together with previous surveys reveals that this N-trending folding is believed to be related to the inversion of the Jurassic and Early Cretaceous pre-existing fault zones and generated in response to the late compressive deformations. In addition, the study area provides evidence of soft-sediment deformations by good exposures of Cretaceous-aged slump sheets. Slump folds are usually associated with several meso-scale syn-sedimentary normal faulting together with frequent reworked blocs and occasional conglomeratic horizons. All these features indicate sedimentation on irregular seafloor topography. The aim of the present study is to investigate slump folds by applying techniques to reconstruct the contemporaneous slope gradient which has triggered soft-sediment deformations. Moreover, the brittle deformation is quantified using fault kinematic analysis together with the analysis of lithostratigraphic correlation and syn-sedimentary structures. Considerable thickness variations of Cretaceous deposits are interpreted as controlled by normal faulting activities. Likewise, fault kinematic analysis typifies a regional pure extension that trends NNW during Barremain, NNE during Albian and probably NW during Cenomanian time. Based on slump folds analysis, the inferred sub-marine paleoslope is believed to have a northward dipping during Barremian and a NNE-dipping during Albian time. On the light of the over-mentioned interpretations, it is believed that Cretaceous sedimentation of the study area is highly controlled by major syn-depositional normal faults associated with intra basin growth faulting. These fault systems seem to be related to the Southern Tethyan expansion of the rifted continental passive margin.

Keywords: Slumping, Submarine paleoslope, Fault Kinematics analysis, Northern Tunisia, Cretaceous.

1. Introduction

Slumping is one of the most common features that characterize gravity-driven structures, dealing with unlithified sediments above an irregular basin floor. Slump folds seem to be the most significant deformation reflecting downslope flow (Strachan and Alsop, 2006). These soft-sediment deformations reflect the orientation of the palaeoslope. Many paleogeographic reconstitutions can be recognized using the systematic and meaningful link between slump folds distribution and the sub-marine paleoslope attitude above which they were initially triggered (Woodcock, 1979; Strachan and Alsop, 2006; Debacker and De Meester, 2009; Alsop and Wenberger, 2020). After the pioneering work of Jones (1940), many studies have investigated the soft-sediment deformations and described a lot of statistical methods which have been applied in a number of settings to deduce the paleoslope dip direction from slump features (Hansen, 1965, 1967; Woodcock, 1979; Bradley and Hanson, 1998; Strachan and Alsop, 2006; Strachan, 2008; Debacker and De Meester, 2009; Debacker, 2012; Alsop and Marco, 2011, 2012a, b, 2013, 2014; Yong and al., 2013; Sharman et al., 2015).

Submarine mass-movement within the Cretaceous sequences of Borj Cedria provides a well-exposed example of soft-sediment deformation patterns within slump sheet. The Cretaceous sub-marine slumping of this area is related to the Southern Tethyan rifted continental margin evolution (Marie et al., 1982; Turki, 1985; Martinez et al., 1990; Saadi, 1990). Thus, during the rifting stage, major growth faulting is highlighted which is responsible for basin floor instability. Consequently, many slope failures occur on top of which incoherent sediments move downwards due to their pure gravity and/or seismic activity (Strachan and Alsop, 2006; Alsop et al., 2013; Sharman et al., 2015). A large spectrum of mass transport deposits is described related to slope gradient degree (Strachan, 2006; Alsop and Marco, 2011, 2012a, b; 2014; Sharman et al., 2015). The mechanisms of the gravity-driven deformational features are still poorly known or even not well characterized in this area and the basin architecture is classically studied only on the basis of stratigraphic and/or sedimentologic tools (Bey et al., 2012; Amri et al., 2018).

This paper aims to explore a good number of structural features in order to drawback the Cretaceous basin architecture. Therefore, the main goal is to determine the sub-marine paleoslope direction from slump features on the basis of the genetic link between the original slope and slump fold distribution. Lithostratigraphic correlations together with detailed syn-sedimentary structures analysis are also used to infer the palesoslope direction. Furthermore, the brittle deformation, which reflects the paleostress state, is quantified through the kinematic analysis of syn-sedimentary fault populations.

2. Geologic setting

The study area belongs to the northeastern part of Tunisia, located close to the gulf of Tunis (Fig. 1). Tunisia corresponds to the far northeastern part of the NE-trending Atlas belt structured by continuous compressions between the African and Eurasian plates during Cenozoic time (e.g., Guiraud, 1998; Frizon De Lamotte et al., 2002; Stampfli et al., 2002). The Tunisian Atlas system belongs to the eastern part of the Alpine belt of Africa known as the "Maghrebides Chain". Except for its far northern side which belongs to the Numidian thrusted domain, the northern Tunisian Atlas is commonly divided into two well-known structural entities (Fig. 1):

The Borj Cedria-Bou Kournine studied area is affiliated to the Zaghouan–Ressas thrust which constitutes the southern front of the Tunisian Alpine province. This first unit is bounded by a reverse inherited major fault. During Mesozoic times, this large-scale faulting forms a paleogeographic borderline separating a relatively southward shallow marine platform from a northward deep marine basin (Burollet, 1956, Morgan et al., 1998; Soua, 2016).

The second one corresponds to the major Teboursouk thrust entity which marks the northern front of the Alpine domain. This second unit is composed of a large number of salt structures belonging to the northeastern Maghreb salt province (Masrouhi et al., 2013; Jaillard et al., 2013a, b, 2017).

During the Mesozoic times, the Tunisian realm is subjected to a continuous geodynamic expansion of the northern Atlas chain. Primarily, a Mesozoic rifting took over the Permian passive continental margin of North Africa (Frizon de Lamotte et al., 2015) that extended to the Early Cretaceous (Guiraud, 1998; Rosenbaum et al., 2002; Stampfli et al., 2002; Bouaziz et al. 2002; Soussi, 2003; Guiraud et al. 2005; Gharbi et al., 2013). From the latest Cretaceous to the present, a compressional tectonic stage is highlighted with shortening tectonic episodes interrupted by relative tectonic quiescence periods (Guiraud and Bosworth, 1997; Frizon de Lamotte et al. 2002; Masrouhi et al., 2008).

The rifting phase occurring during the Early Mesozoic time has resulted in Triassic mini-basins dominated mainly by thick beds of evaporites, dolomites and clays reflecting epicontinental depositional environment (Snoke et al., 1988; Kamoun et al., 2001; Soussi et al., 2017), overlaid by Jurassic carbonate layers which were deposited during the Tethyan rifting (Soussi, 2003; Boughdiri et al., 2007). From the Jurassic to early Cretaceous, major extensional tectonic events predominated in relation with the breakup of the Central Atlantic (Snoke et al., 1988; Souquet et al., 1997; Soussi et al., 2000; Boughdiri et al., 2007; Masrouhi and Koyi, 2012; Bahrouni et al., 2016; Dhahri and Boukadi, 2017, Naji et al., 2018a). This extensional episode is responsible for the dislocation of the continental platform resulting in considerable synsedimentary normal faults creating tilted blocks basin architecture. Accordingly, this basin configuration is characterized by irregular sea-floor topography, responsible for thickness and/or facies variations, abundant slumps sheets within syntectonic early

Cretaceous sequences (Snoke et al., 1988; Guiraud et al. 2005; Soua et al., 2009; Gharbi et al., 2013; Masrouhi et al., 2014b; Jaillard et al., 2013; 2017; Naji et al., 2018a, b). During early Cretaceous times, this extensional tectonic regime was accompanied along this margin by hyperactive halokinetic movements (Masrouhi et al., 2013; Dhahri and Boukadi, 2017, Jaillard et al., 2017; Belkhiria et al., 2017). Furthermore, by locality, volcanic activity recognized by basaltic flows was described as the result of rift-related magmatism. (Mattoussi Kort et al., 2009). These particular features (both halokinetic and volcanic activities) characterize the Tethyan passive margin style (Mattoussi Kort et al., 2009; Dhahri and Boukadi, 2017, Jaillard et al., 2017). In addition, the late Aptian to the lower-middle Albian period is characterized by the most extensional event of the south Tethyan margin in northern Tunisia (Souquet et al, 1997; Masrouhi et al., 2014b, Naji et al, 2018a, b; Amri et al., 2020). A paleogeographic differentiation between platforms in central and southern areas (Gharbi et al., 2013) and a deep trough in the northern area is implied (Burolet, 1956). Moreover, during the same period, relevant Cretaceous halokinesis indicated thick and/or thin-skinned tectonic extension (Slama et al., 2009; Masrouhi and Koyi, 2012; Amri et al., 2020). The early to middle Albian is perceived to coincide with the final stage of Atlantic Ocean opening (Jaillard et al., 2013a, b). The late Cretaceous corresponds to an extensional post-rift cycle characterized by shallow marine carbonate and open marine shale sedimentation. Subsequently, the deposition during this period is essentially controlled by the isostatic response of successive depocenters and/or major faults disposition (Gharbi et al., 2013; Naji et al., 2018a, b). A compressional phase, subsequent to the Mesozoic rifting, has started since the Senonian time (Maastrichtian?). It is related to African/Eurasia plates' convergence, inducing the Tethys seaway closure and the positive inversion of the basin (e.g. Chihi, 1995; Gharbi et al., 2015; Masrouhi et al., 2019; Guiraud and Bosworth, 1997).

3. Dataset and approach

To study the tectono-sedimentary pattern along the northeastern Tunisia (Borj Cedria case study) and deduce related paleoslopes orientations during Cretaceous time, lithostratigraphic correlation, geological mapping together with field data collection (slump folds, directional syn-sedimentary structures and fault kinematic analysis) are carried out. Subsequently, paleoslope orientation from slump folds and sedimentary structures dataset is deduced using Stereonet 9 plotting software (Cardozo and Allmendinger, 2013; Allmendinger et al., 2013). Moreover, the fault kinematic analysis and paleostress reconstructions are made using Win-Tensor computer software (Delvaux and Sperner, 2003, Delvaux, 2016).

To start with, the fault kinematic analysis yields important information about the brittle deformation. Such analysis provides a main description of the reduced stress tensor consisted of the related trends of the three principal stress axes (σ1, σ2, σ3) with the stress ratio (R). Three tectonic regimes

(extensional, strike-slip or compressional regime) are distinguished based on the vertical principal stress. The relationship between the three stress orientations σ1, σ2 and σ3 is illustrated by the stress ellipsoid and can be given by the stress ratio R ranging from 0 to 1 and denoted as following: R = (σ2 - σ3)/(σ1 - σ3) (Angelier and Goguel, 1979; Sperner and Ratschbacher, 1993; Ritz and Tobaoda, 1993; Bellier and Zoback, 1995). Here, the study area exposes a large number of sealed normal faults in which related fault displacement and type are recorded on fault mirrors. However, in some cases, fault planes show different families of striae. In such conditions, the separation of generations (slip vectors) is made by referring to structural arguments using relative chronology of the striations (i.e., crosscutting relationships) together with their relations with regional recognized tectonic phases. Specifically, meso-scale sealed syn-sedimentary faults have been especially surveyed here, because they directly provide the date of the tectonic event. Collected from Borj Cedria outcrops, the fault datasets are processed to deduce the paleostress tensor on the basis of the "Right Dihedron method" (Angelier and Mechler, 1977; Tranos, 2017) and/or the Optimum methods (Delvaux et al., 2012). Moreover, It is important to note that all fault datasets need to be tilted back to their original horizontal orientation in order to assume the initial stress tensors.

On the other hand, the ductile deformation is highlighted using slump folds investigation based on the assumption that the distribution of slump deformations has been correlated to the orientation of the underlying sub-marine slope (Fig. 2A). Jones (1940) was the first geoscientist who carries out this perception through the Mean Axis Method (MAM) based on the affiliation between the mean slump fold axis and the related paleoslope orientation (Fig. 2B). Later, geoscientists have been interested in the study of soft-sediment deformations and they described different methods for deducing paleoslope dip direction from slump folds (e.g. Hansen, 1965, 1967; Woodcock, 1979; Bradley and Hanson, 1998; Alsop et al., 2001; Strachan and Alsop, 2006; Strachan, 2008; Debacker and Meester, 2009; Debacker, 2012; Yong et al., 2013; Alsop and Marco, 2011, 2012a, b, 2013, 2014; Sharman et al., 2015). In the present study, the paleoslope analysis using slump folds is conducted on the basis of two methods: the Mean Axis Method (MAM) and the Axial-Planar Method (APM) (Fig. 2B). The first one (Mean Axis Method) originally developed by Jones (1939), and later reviewed by Woodcock (1976b) who postulated that slump fold axis may develop at right angles to the downslope orientation and recognized statistical arrangement perpendicular to the flow or slump sheet trending. Thus, this first method suggests two hypothetical transport directions which are diametrically opposed. Subsequently, the paleoslope dip direction is commonly selected by referring to the regional known paleogeographic stress (Jones, 1939, Woodcock, 1976b), and/or on the basis of the vergence of slump features (Woodcock, 1976b). Furthermore, it should also be noted that slump folds measurements or at least the deduced paleoslope orientation need to be tilted back to their original orientations in order to remove later tectonic deformations. Otherwise, this method

(MAM) has the advantage of being statistically powerful as a result of being based on average properties of fold measurements. However, the main inconvenient of this method that it does not work with downslope (Fig. 2C) where slump axes are trending in parallel or oblique to the flow orientation (Woodcock, 1979; Strachan and Alsop, 2006; Alsop and Holdsworth, 2007). The second method called the Axial-Planar Method (APM) uses the fold axial planes which provide significant kinematic perception in the same way as slump axes (Woodcock, 1976a, 1976b; Woodcock, 1979; Sharman et al., 2015).Subsequently, the poles to axial surfaces have tendency to range in a great circle around the mean fold axis, and consequently the strike of the best-fit girdle to these poles yields a bi-directional indication of slumps flow orientation (Woodcock, 1976b, Sharman et al., 2015). Moreover, the imbrication of the mean axial plane respectively to the general slumps flow trending may be used to deduce the original slope orientation (Woodcock, 1976b).

4. Tectono-sedimentary dataset

4.1. Lithostratigraphy of the study area and correlation of measured sections

The study area (Fig. 1) shows well-exposed outcrops of Mesozoic and Cenozoic series which are easily recognizable and accessible. In this section, detailed Cretaceous lithostratigraphic description and correlation between the study area and surrounding fields are made (Fig. 3) on the basis of the current investigation with previous studies (e.g. Turki, 1985; Ouahchi et al., 1993; Morgan et al., 1998).

The Barremian to Aptian successions exposed in northeastern Tunisia have an estimated thickness of about 2500 meters in Jebel Oust which is considered as a potential reference section for the early Cretaceous (Souquet et al., 1997). The early Cretaceous outcrops of northeastern Tunisia have been usually characterized as “flyschoid deposits” which are mostly made of continuous alternation of sandstone beds and shale layers deposited in a deep-water environment. The turbidite, carbonate breccia and conglomeratic layers are often found that indicate syn-tectonic activities (Memmi, 1981, 1989; Souquet et al., 1997; Naji et al., 2018b).

In the study area, situated 30 km to the northeast of Jebel Oust, The Jurassic and lower Cretaceous lithofacies include reefs and bioclastic limestone beds associated with syn-tectonic soft-sediment deformations, intraformational breccias and debris flows (Cossey and Ehrlich, 1978; Marie et al., 1982; Turki, 1985; Morgan et al., 1998). Several authors (Cossey and Ehrlich, 1978; Marie et al., 1982; Turki, 1985; Soussi, 2003) have postulated the presence of submerged paleohigh developed in the top the Bou Kournine-Ressas tilted block around the Jurassic-Cretaceous transition. During Barremian-Albian period, this area corresponds to a reef platform domain and the depositional environment is mainly marked by gravity tectonics (Marie et al., 1982; Turki, 1985; Martinez et al., 1990). The geodynamic context of this period appears to be guided essentially by N45 and E-W

trending normal faulting (Turki, 1985). Furthermore, the preserved tectono-sedimentary markers correspond to olistolithes, monogenic breccias and slumping sheets encountered in the Barremian and Albian deposits of Borj Cedria area. The Cenomanian-Turonian sedimentation is characterized by para-reef bioclastic limestone (Isis Member), deposited in an outer platform (Marie et al., 1982). To the east, considerable thickening of the reef deposits is described, particularly in the Gulf of Hammamet area (Sebei et al., 2019), before grading into clays with planktonic microfauna in the Cap-Bon, characteristic of open sea (Marie et al., 1982). Moreover, the geodynamic context of the late Cretaceous period exhibits the reactivation of inherited faults. Thus, Early Cretaceous E-W trending faults seem to be reactivated as dextral-normal movement in the study area. The sedimentation is controlled essentially by N40 and N140 trending syn-sedimentary normal faults separating subsiding zones with high rate of sedimentation from paleohigh zones characterized by condensed late Cretaceous series (Turki, 1985; Martinez et al., 1990).

The lithostratigraphic correlation established between Jebel Mekki in the South and Jebel Bou Kournine-Borj Cedria in the North highlights significant northward thickening of Barremian-Santonian series clearly showing tilted blocks geometry (Fig. 3). Then, Barremian sequences, composed of marly-nodular limestone alternating with siliciclastic sandstone beds, shows a considerable thickness increase from Jebel Mekki to Jebel El Khourrija (Fig. 3). On the one hand, this thickness variation is believed to be linked to E-W-trending normal faults activities. On the other, the Barremian beds exposed in Bou Kournine-Borj Cedria area and Jebel El Khourija structure are equal in thickness. The Barremian sequences of Bou Kournine-Borj Cedria show large number of syndepositional structures with frequent slump folds generated by syn-tectonic extensional activity. In this area, the Aptian-Albian deposits are composed of gray to black marls and alternating limestone and discrete sandstone beds. These deposits include slump sheets and show a northward thickness increase. During the late Cretaceous, the siliciclastic input became reduced and sedimentation was going to be more uniform generally composed of marl and fine grained limestone beds. From Jebel Mekki to Jebel Bou Kournine, a northward thickening of the late Cretaceous deposits has been perceived (Fig. 3).

4.2. Analytical results illustrating the synsedimentary faulting

In the current study, field survey has been conducted to investigate fault kinematic analysis that yields significant information about the paleostress tectonic regime. Our study area (Fig. 4A) exposes multiple Cretaceous meso-scale synsedimentary faults with well-preserved brittle tectonics indicators (Fig. 4). Syndepositional striated faults are especially surveyed in order to deduce tectonic regime during Barremian, Aptian and Cenomanian-Turonian intervals.

4.2.1. Barremian tectonic regime

The Barremian sequences display evidence for conglomerate-rich and slumped beds in addition to frequent syn-sedimentary meso-scale normal faults (Fig. 4B and C). Therefore, numerous faults datasets are collected from Barremian deposits and rotated to their primitive orientation in order to restore their initial tectonic regime. As a result, the computed stress tensors corresponding to this area reveals a mostly uniform stress field. In this regard, four sites are processed and provide a pure extensional tectonic regime with a general WNW to NNW trending during this period. In more details, back-tilted fault diagrams of three sites (Fig. 5, S1, S4 and S5) exhibit a stress tensor showing a NNW-trending extensional tectonic regime. However, the analysis of fault population of the only remaining site (Fig. 5, S3) illustrates extension that trends WNW-ESE.

4.2.2. Aptian-Albian tectonic regime

The study of Aptian-Albian deposits reveals frequent ~NW-SE and NE-SW trending meter-scale sealed normal faults (Fig. 4D and E). The processed striated fault planes clearly provide that the predominant paleostress regime in the study area shows a general NNE to NE-trending extension. Five sites are consequently analyzed to deduce the Aptian-Albian paleostress regime. In details, four sites (Fig. 5, S6, S78, S11 and S12) reveal a pure extensional tectonic regime with a stress tensor characterized by NNE-trending. Whereas unfolded fault measurements of the remaining site (Fig. 5, S13) illustrate similar pure extensional regime with NE-trending stress tensor.

4.2.3. Cenomanian-Turonian tectonic regime

The Cenomanian-Turonian outcrops show remarkable synsedimentary extensional features (reworked blocks, nodules, olistolithes...etc.) associated with meso-scale sealed normal faulting (Fig. 4F). Due to poor quality of outcrops, inaccessibility and observation gaps, a small number of striated faults datasets is collected. Despite this, an extensional tectonic regime with NNW-SSE trending is highlighted (Fig. 5, S9).

4.3. Analytical results illustrating the regional stress tensor

A comprehensive investigation of regional stress field along Borj Cedria-Bou Kournine faulted area was highlighted in the current study. Striations measured on fault planes are used to characterize the regional stress regime. Therefore, graphical methods have been here used to separate heterogeneous data sets and eliminate non-linear measurements.

The study area is believed to be controlled by a persistent extensional tectonics related to the Cretaceous Tethyan rifting (Turki, 1988; Ouahchi et al., 1993; Morgan et al., 1998). Likewise, the inversion of 12 Barremain-aged fault data inputs indicates clear NNW-extensional tectonic regime.

In details, the corresponding back-tilted faults diagram illustrates horizontal NNW-trending minimum stress tensor σ3 (03/342) and a stress ratio R=0,50. The σ1 axis of this stress regime has high angle trending WNW-ESE- (83/097), the intermediate σ2 stress trends ENE-WSW and shows 06/252 stress

axis (Fig. 6). Furthermore, 14 striated fault mirrors collected throughout well-exposed Albian sequences across the Bou Kournine-Borj Cedria area are processed. Subsequently, the unfolded faults diagram illustrates clearly NNE-SSW extensional tectonic regime according to the following parameters: a stress tensor shows a gently plunging NNE-trending minimum stress axis (02/030) and WNW-trending near-horizontal intermediate stress axis (00/300). The maximum stress tensor displays a high dip angle and SSW-trending σ1 (88/199). This fault population indicates a stress ratio R=0.46 (Fig. 6).

4.4. Slumps analysis results

In the study area, Barremian and Albian sequences give evidences for well-developed soft-sediment deformation structures which are highly related to the expansion of the Southern Tethyan rifted continental passive margin (Masrouhi et al., 2014b; jaillard et al., 2017; Naji et al. 2018a,b). The slumping, particularly generated in pre-existing mud-rich deposits, is the most typical kind of gravity-driven sediment transport processes that reflect the slope attitude and the basin-floor topography.

In the current study, 21 meso-scale slump folds are collected throughout the Barremian sandy limestone strata of the Bou Kournine-Borj Cedria area (Fig. 7). The most observed slump folds geometry is described as asymmetric folds with thinner long limbs and thicker short limbs. This assessment gives a preliminary idea about the transport direction (Fig. 7D). “Mean Axis Method” and “Axial Planar Method” are rigorously applied for the collected Barremian slumps folds. Consequently, both techniques give close values within a general northward dipping sub-marine paleoslope. The analysis of restored slump axis (MAM method) highlights ~N008-trending paleoslope, whereas the back-tilted poles to axial planes (APM method) show comparable value of ~N002-dipping paleoslope (Fig. 7G).

The Albian deposits similarly show soft-sediment slumps related to the Cretaceous extensional tectonic that occurred in the north-eastern Tunisia (Naji et al., 2018a). Abundant decametric slump folds associated with frequent re-sedimented blocks and calcareous nodules are described within Albian green-black marls series alternating with marly nodular limestone beds (Fig. 8). These features are considered to be derived from gravity flows along a submarine paleoslope. Therefore, a good number of Albian slump folds are measured and computed using the two methods (MAM and APM) and illustrate a general ~NNE-dipping sub-marine paleoslope. More precisely, the restored slump axis method illustrates a paleoslope orientation of ~N26 and the unfolded poles to axial planes give a value of ~N34-trending (Fig. 8G). Consequently, along the study area, the deduced paleoslope dipping provides a persistent irregular basin floor. Likewise, the inherited early Cretaceous ~E-W trending faults system seems to remain active during Albian period in conjunction with synsedimentary ~NNW to ~NW trending normal faulting.

4.5. Analytical results illustrating paleocurrent direction

The early Cretaceous flysch deposits of Borj-Cedria area provide evidence for abundant centimetric to decimetric “olistostromes” reworked blocks (Fig. 9d) associated with syntectonic comglomeratic horizons which testify to active normal growth faulting. In addition, early Barremian sequences highlight numerous directional syn-sedimentary structures (Fig. 9a, b, c, e) indicating a shallow marine deposition. A paleocurrent analysis is rigorously performed through the examination of these different Barremian-aged sedimentary structures (particularly flute and groove marks). The inferred rose diagram (Fig. 9f) shows the result of the analysis of 17 rotated measurements and illustrates a clear northward paleocurrent orientation. The latter seems to be persistent across the entire area in the Barremian times. The result is correlated to slump fold analysis and consequently confirms the regional northward Barremian paleoslope orientation.

5. Discussion

The fold-and-thrust belt of the Northern Tunisia observed at the present-day is the result of complex tectonic expansion of the northern African margin which began with the late Permian break up of Pangea and ended with the Cenozoic Alpine orogeny.

5.1. Mesozoic paleoslope reconstruction of Borj Cedria-Bou Kournine area

The geodynamic evolution of the northern margin of Africa has been mainly guided by the extension, the crustal stretching and thinning, as well as subsidence during the Mesozoic Tethyan rifting (Boughdiri et al. 2007; Mattoussi Kort et al., 2009; Gharbi et al. 2013; Soussi et al. 2017; Naji et al. 2018a,b). During the Jurassic and early Cretaceous period, the dislocation of the continental platform in relation with the opening of Central Atlantic (Fig. 10A, B, C) is responsible for the creation of major synsedimentary normal fault systems developing tilted blocks basin architecture (Martinez et al., 1991; Snoke et al., 1988, Souquet et al. 1997; Piqué et al., 2002; Guiraud et al., 2005; Boughdiri et al. 2007; Masrouhi and Koyi 2012; Masrouhi et al., 2013; Gharbi et al., 2013; Tlig et al., 2015, Naji et al., 2018b). A similar Mesozoic structural configuration with correlative extensional structures is recorded in the northern range of the Tethyan margin including the Adria microplate (Masse and Borgomano, 1987; Bertok et al., 2012; Santantonio et al., 2013; Tavani et al., 2015).

In northern Tunisia, the Jurassic and earliest Cretaceous sedimentation was controlled by E-W normal faulting, created in response to a general N–S extension (Bouaziz et al., 1999, Piqué et al., 2002). The inherited faults oriented NE–SW, NW–SE and N–S, were also active over the same time (Piqué et al., 2002). The Jurassic series are largely composed of thick mass-transport deposits separated by turbidite sequences (Fig. 10D). Therefore, the Jurassic depositional environment is mainly guided here by major E-W growth faulting activities that control a northward regional paleoslope (Fig. 10A) above which multiple soft-sediment deformations were triggered (Cossey and

343 Ehrlich, 1978). In addition, early Cretaceous deposits, outcropping in northern Tunisia, show
344 increased thickness and locally facies variations. It also display numerous soft-sediment
345 deformations, slumping, reworked blocks and syntectonic growth strata that are believed to be
346 coeval with the southern Tethyan rifted continental passive margin geodynamic evolution (Gharbi et
347 al., 2013; Naji et al., 2018a,b). In this regard, the Barremian deposits across the Bou Kournine-Borj
348 Cedria area provide evidence for numerous meso-scale slump folds (Fig. 7) associated with frequent
349 metric sealed normal faults. The turbiditic layers associated with frequent sandstone beds, show
350 directional sedimentary structures including hummocky cross stratifications (HCS), flute casts, groove
351 marks...etc., (Fig. 9) are here highlighted. The deposition of HCS structures requires careful
352 consideration of the possible ways that storm waves (oscillatory current) and turbidity current
353 (unidirectional current) interact both in time and space. Consequently, the HCS trigger is highlighted
354 to occur in proximal setting where the gradient of the slope is slightly inclined (Lamb et al., 2008). In
355 distal setting where slope gradient increases, the lack of oscillatory current flow leads to flute and
356 groove marks generation which reflects a unidirectional flow (Lamb et al., 2008). Thus, the
357 compilation of all these over-mentioned observations suggests for sedimentation above an irregular
358 basin floor under an extensional tectonic regime. A clear syn-rift Barremian tectonic style is likewise
359 highlighted.
360 The fault kinematics obtained from the analysis of unfolded striated fault mirrors collected from the
361 Barremian strata of the study area, display evidence for clear regional NNW-trending extensional
362 tectonic regime during this period. In addition, the back-tilted stereoplot shows frequent NE, NNE
363 and WNW-trending Barremian faults (Fig. 6). Using slump fold analysis, the unfolded slump axis and
364 poles of axial planes (MAM and APM respectively) illustrate very close results with a general
365 ~northward dipping sub-marine paleoslope during Barremian time (Fig. 10B). The same result is
366 confirmed through the paleocurrent indicators datasets (Fig. 9). In order to explain the ~N-S trending
367 of syn-sedimentary normal faulting which is here contemporaneous with the northward facing
368 paleoslope during the Barremian, two assumptions are here proposed. The first one suggests an
369 inherited ~E-W major fault situated to the south of the study area (probably between Jebel Bou
370 Kournine and Jebel Ressass), created during the Jurassic-earliest Cretaceous times that controls a
371 regional northward dipping paleoslope. The second assumption suggests a possible southward
372 located diapiric intumescence responsible for the northward dipping paleoslope during the
373 Barremian time. In this way, the southward Jebel Ressass structure is considered to be a salt diapir
374 developed during Cretaceous period (Jammeli et al., 2011; Turki, 1985; Martinez et al., 1990). In this
375 case, the extensive slumping is believed to be the result of salt intrusion which has fractured and
376 oversteepened the slope leading to instability and failure of the basin floor (Alsop et al., 2001; Alsop
377 and Holdsworth, 2007).

The Aptian - Albian time interval has long been recognized as the most extreme extensional period characterizing the South Tethyan margins including the major part of northern Tunisia platform which was broken up by active halokinesis (Martinez et al., 1991; Snoke et al., 1988; Souquet et al., 1997; Vila et al, 1998; Piqué et al., 2002; Gharbi et al., 2013; Masrouhi et al., 2013; Jaillard et al., 2017). Likewise, due to intense extensional tectonics, several widespread salt structures are documented as having grown during the Aptian–Albian period which is also perceived to have deposited the thick and rapid sedimentation rates (Souquet et al., 1997; Vila et al, 1998; Masrouhi et al., 2014b; Jaillard et al., 2017). Some salt structures probably dominated by raft tectonics on submarine salt bodies, especially active during the Albian time (Vila et al, 1998). The early to middle Albian extension was correlated with the final stage of Atlantic Ocean opening (Jaillard et al., 2013). In northern Tunisia, the sedimentation becomes more and more homogeneous since the Aptian-Albian which is mainly made of limestone beds alternating with marls (Fig. 10D). In addition, Aptian-Albian sequences show significant thickness variation with frequent sealed decametric normal faults associated with abundant slump sheets. In this context, fault kinematic is obtained from the analysis of restored fault, display evidence for homogenous paleostress tensor with a general ~NE-trending pure extension (Fig. 6). More specifically, the MAM and APM methods typify very comparable results within a general ~NNE-dipping sub-marine Albian paleoslope orientation (Fig. 10C). Based on these findings, the Aptian-Albian sedimentation seems to be mainly controlled by NW to NNW-trending normal faults (Fig. 6), in agreement with previous results (Turki et al., 1988, Piqué et al., 2002). In addition, the unfolded Cenomanian fault diagram illustrates NW-trending extensional tectonic regime. From the Cenomanian to the Campanian, the pelagic to hemipelagic depositional environments were widely distributed, guided mainly by the isostatic response of major fault systems and/or depocenters, developed during an extensional period of post-rift stage (Gharbi et al., 2013; El Amari et al., 2016; Naji et al, 2018a, b).

5.2. Present-day configuration of Borj Cedria-Bou Kournine area

The northern Atlas domain of Tunisia is characterized by numerous NE-trending Atlassic folds (classically called the “Atlassic direction” in the literature) resulting from the major northwest-trending Mid-Miocene tectonic compression (Ben Ayed, 1986; Chihi, 1995; Bouaziz et al., 2002; Masrouhi et al., 2019; Khomsi et al., 2019). Although, the study area exposes sub-meridian fold belts (Fig. 1). This N-S trending folding is highlighted in some other localities from northern Atlassic domain of Tunisia including Jebel Naheli (Ben Ayed, 1986), Jebel Touila located in the Nebeur area (Chikhaoui, 1988)…etc. In addition, two principal major fault populations are highlighted across the study area (Fig. 1): (1) A N-S trending faults which divide the region into several blocks probably created during the Barremian; (2) A NW-trending faults located in the southern and northern parts of the field and which seem to control the sedimentation during the mid to late Cretaceous.

Subsequently, a stress field perturbation is observed to the right of N-S trending major faults and an E-W contraction has acted during the general NW-trending Alpine Cenozoic compression as previously mentioned by Martinez et al., 1990. This assumption is based on numerous field observations including shear planes striae, schistosity, bench on bench sliding, stylolitic peaks…etc. In addition, NW-trending faults which delineate this area are responsible for movements toward the south-east (Turki, 1985; Martinez et al., 1990).

A second structural complexity of the study area lies in the fact that Jurassic limestones are thrusted in normal position over the Cretaceous deposits. The Jurassic series are now at 570 m of elevation (Fig. 10D). Based on lithostratigraphic and structural affinities, it is believed that Jurassic deposits have been elevated up here at least 1500 m above their original position. The thickness and facies variations characterizing the Jurassic and Cretaceous series of the study area indicate that Mesozoic sedimentation was controlled by active extensional setting. Subsequently, such variations have guided the style and the position of the major subsequent thrusting (Turki, 1988; Martinez et al., 1990; Souquet et al. 1997; Morgan et al. 1998). In addition, previous studies of Turki, 1985; 1988 highlights the involvement of the Triassic evaporites in the main thrust fault. Therefore, all the above-mentioned features are in favor of fault systems inversion model for the development of the major faults of the study area as it was drawn on the cross section of the Fig. 10D. This cross section illustrates the present-day structural configuration of Borj Cedria-Bou Kournine area. It shows clearly reverse pre-existing Jurassic and early Cretaceous normal faulting systems. The basement detached fault within the Triassic deposits is believed to be the continuity of the present day major Zaghouan thrust fault.

6. Conclusion

The Cretaceous outcrops of Bou Kournine-Borj Cedria area, Northern Tunisia, exhibit multiple soft-sediment deformations related to major synsedimentary normal faulting that was responsible for irregular basin geometry. This architecture is marked by variable paleoslope distribution in context of the Tethyan rifted continental passive margin. Subsequently, the lithostratigraphic correlation established in the current study illustrates a significant thickness variation of the Cretaceous series due to both inherited and syn-depositional growth normal faulting activities. The results are summarized as follows:

1) Fault kinematic analysis of Barremian striated planes typifies NNW-trending regional extensional tectonic regime. 2) Slump folds together with directional sedimentary structures analysis testify a general northward dipping sub-marine Barremian paleoslope. 3) During the Aptian-Albian period, the study area seems to be controlled by NNE-trending regional extensional tectonic regime. 4) Using slump fold analysis methods, an Albian ~NNE-dipping sub-marine paleoslope is depicted. 5) The N-

trending folding is believed to be related to the pre-existing fault zones and generated in response to the late compressive deformations.

Acknowledgments

The authors would like to thank the Editor-in-Chief Pr. Abdullah M. Al-Amri. We are grateful to the Editor Pr. François Roure and both anonymous reviewers for their helpful and insightful comments that greatly contributed to improving this paper.

Funding and/or Conflict of interests/Competing interests

This work was financially supported by the Tunisian Ministry of Higher Education and Scientific Research (CERTE, Geo-resources Laboratory funding). We wish to draw the attention of the Editor that the authors have no conflicts of interest to declare. All co-authors have seen and agree with the contents of the manuscript.

References:

Allmendinger, R.W., Cardozo, N.C., Fisher, D., 2013. Structural Geology Algorithms: Vectors & Tensors. Cambridge University Press, Cambridge, England, 289.

Alsop, G. I., Bryson, R., Hutton, D. H. W., 2001. Tectonic and kinematic evolution within mid-crustal orogenic root zones: a case study from the Caledonides of northwestern Ireland. Geological magazine, 138 (2), 193−211.

Alsop, G.I., Holdsworth, R.E., 2007. Flow perturbation folding in shear zones. In: Ries, A.C., Butler, R.W.H., Graham, R.D. (Eds.), Deformation of the Continental Crust: The Legacy of Mike Coward: Geological Society, London, Special Publications, 272, pp. 77–103.

Alsop, G. I., Marco, S. 2011. Soft-sediment deformation within seismogenic slumps of the Dead Sea Basin. Journal of Structural Geology, 33, 433-457.

Alsop, G. I., Marco, S., 2012b. Tsunami and seiche-triggered deformation within offshore sediments. Sedimentary Geology, 261–262, 90–107.

Alsop, G.I., Marco, S., 2012a. A large-scale radial pattern of seismogenic slumping towards the Dead sea basin. Journal of the Geological Society, 169, 1, 99-110.

Alsop, G. I., Marco, S., 2013.Seismogenic slump folds formed by gravity-driven tectonics down a negligible subaqueous slope. Tectonophysics, 605, 48−69.

Alsop, G.I., Marco, S., 2014. Fold and fabric relationships in temporally and spatially evolving slump systems: A multi-cell flow model. Journal of Structural Geology, 63, 27–49.

Alsop, G. I., Weinberger, R., 2020. Are slump folds reliable indicators of downslope flow in recent mass transport deposits?. Journal of Structural Geology, 135, 104037.

Angelier, J., Mechler, P., 1977. Sur une méthode graphique de recherche des contraintes principales également utilisable en tectonique et en séismologie: la méthode des dièdres droits. Bulletin de la société géologique de France, 19, 1309–1318.

Angelier, J., Goguel, J., 1979. Sur une méthode simple de détermination des axes principauxdes contraintes pour une population de failles. C. R. Acad. Sci. 282, 307–310.

Amri, A., Fadhel, M. B., Chermiti, A., Youssef, M. B., 2018. Biostratigraphy of upper Cretaceous through Paleocene successions in Grombalia, Tunisia (southern Tethyan domain)—reworking processes and interpretations. Arabian Journal of Geosciences, 11: 253.

Amri, Z., Naji, C., Masrouhi, A., Bellier, O., 2020. Interconnection salt diapir–allochthonous salt sheet in northern Tunisia: The Lansarine–Baoula case study. Journal of African Earth Sciences, 170, 2020, 103876.

Bahrouni, N., Houla, Y., Soussi, M., Boughdiri, M., Ali, W.B., Nasri, A.,Bouaziz, S., 2016. Discovery of Jurassic ammonite-bearing series in Jebel Bou Hedma (South-Central Tunisian Atlas): Implications for stratigraphic correlations and paleogeographic reconstruction. Journal of African Earth Sciences, 113, 01, 101–113.

Belkhiria, W., Boussiga, H., Inoubli, M. H., 2017. Thick-skinned tectonics within the intracontinental easternmost Atlas foreland-and-thrust belt (Tunisia): Meso-Cenozoic kinematics and implications for regional geodynamics, *Tectonics*, 36, 981– 1004.

Bellier, O., Zoback, M. L., 1995. Recent state of stress change in the Walker Lane zone, western Basin and Range province, United States.Tectonics, 14, 564–593.

Ben Ayed, N., 1986.Évolution tectonique de l'avant-pays de la chaîne alpine de Tunisie, du début du Mésozoïque à l'Actuel. Thèse es Sciences, Paris, Annales Mines Géologie 32, 286p. Editions Service Géologique National Tunisie (1993).

Bertok, C., Capizzi, R., Martire, L., Dela Pierre, F., 2012. The Cretaceous-Eocene succession of the Rocca Busambra (Western Sicily, Italy): a patchy record on a dissected palaeostructural high. Italian journal of geosciences, 131(1), 32-46.

Bey, S., Kuss, J., Premoli Silva, I., Hedi Negra, M., Gardin, S., 2012. Fault-controlled stratigraphy of the Late Cretaceous Abiod Formation at Ain Medheker (Northeast Tunisia). Cretaceous Research, 34, 10–25.

Bouaziz, S., Barrier, E., Soussi, M., Turki, M. M., Zouari, H., 2002. Tectonic evolution of the northern African margin in Tunisia from paleostress data and sedimentary record.Tectonophysics, 357, 227–253 pp.

Boughdiri, M., Cordey, F., Sallouhi, H., Maalaoui, K., Masrouhi, A., Soussi, M., 2007. Jurassic radiolarian-bearing series of Tunisia: biostratigraphy and significance to western Tethys correlations. Swiss Journal of Geosciences, 100, 431–441.

Bradley, D., Hanson, L., 1998. Paleoslope Analysis of Slump Folds in the Devonian Flysch of Maine. The Journal of Geology, 160, 305−318.

Burollet, P.F., 1956. Contribution à l'étude stratigraphique de la Tunisie centrale. Annales des mines et de la géologie, Tunisie, 18, 345 pp.

Cardozo, N., Allmendinger, R.W., 2013. Spherical projections with OSX stereonet.Computers and Geosciences, 51, 193–205.

Chihi, L., 1995. Les fossés néogènes à quaternaires de la Tunisie et de la mer pélagienne: étude structurale et leur signification dans le cadre géodynamique de laMéditerranée centrale. Thèse Doct. Es Science. Géol., Tunis (325 pp.).

Chikhaoui, M., 1988. Succession distension-compression dans le sillontunisien, Secteur de Nebeur, EI Kef (Tunisie centre-nord). Rôledes extrusions triasiques précoces lors des serrages alpins. Thèse Sciences, Univ. de Nice, 143 p.

Cossey, S.P., Ehrlich, R., 1978. Growth fault-controlled submarine carbonate debrisflow and turbidite deposits from the Jurassic of northern Tunisia: possiblecanyon fill sequences. In: Sedimentation in Submarine Canyons, Fans, andTrenches. Stroudsberg, Pennsylvania, Dowden Hutchinson and Ross.

Debacker, T. N., De Meester.E., 2009.A regional, S-dipping late Early to Middle Ordovician palaeoslope in the Brabant Massif, as indicated by slump folds (Anglo-Brabant Deformation Belt, Belgium).GeologicaBelgica, 12, 3-4, 145−159.

Debacker, T. N., 2012.Folds and cleavage/fold relationships in the Brabant Massif, southeastern Anglo-Brabant Deformation Belt.GeologicaBelgica, 15, 1-2, 81−95.

Delvaux, D., Sperner, B., 2003. Stress tensor inversion from fault kinematic indicators and focal mechanism data: the TENSOR program. Geological Society, London, Special Publication, 212, 75–100.

Delvaux, D., 2016. Win-tensor Program (Version 5.8.6 of 23-11-2016), Tensor Program Fault-kinematic Analysis and Tectonic Stress Tensor Inversion.

Dhahri, F., Boukadi, N., 2017. Triassic salt sheets of Mezzouna, Central Tunisia: new comments on late cretaceous halokinesis and geodynamic evolution of the northern African margin. Journal of African Earth Sciences 129, 318–329.

El Amari, A., Gharbi, M., Youssef, M.B., Masrouhi, A., 2016. The structural style of the Southern Atlassic foreland in Northern Chotts Range in Tunisia: field data from Bir Oum Ali Structure. Arabian Journal of Geosciences, 9 (5), art. no. 389.

561 Frizon de Lamotte, D., Bezar, B.S., Bracène, R., Mercier, E., 2002. The two main steps of the atlas
562 building and geodynamics of the Western Mediterranean. Tectonics, 19 (4), 740–761.

563 Frizon de Lamotte, D., Fourdan, B., Leleu, S., Leparmentier, F., de Clarens, P., 2015. Style of rifting
564 and the stages of Pangea breakup. Tectonics, 34 (5), 1009-1029.

565 Gharbi, M., Masrouhi, A., Espurt, N., Bellier, O., Amari, E., Ben Youssef, M., Ghanmi, M., 2013. New
566 tectono-sedimentary evidences for Aptian to Santonian extension of the Cretaceous rifting in the
567 Northern Chotts range (Southern Tunisia). Journal of African Earth Sciences 79, 58–73.

568 Gharbi, M., Espurt, N., Masrouhi, A., Bellier, O., Amari, E.A., 2015. Style of Atlassic tectonic
569 deformation and geodynamic evolution of the southern Tethyan margin, Tunisia.Mar Pet Geol, 66,
570 801–816.

571 Guiraud, R., Bosworth, W., 1997. Senonian basin inversion and rejuvenation of rifting in Africa and
572 Arabia: synthesis and implications to plate-scale tectonics. Tectonophysics, 282, 39–82.

573 Guiraud, R., 1998. Mesozoic rifting and basin inversion along the northern African Tethyan margin:
574 an overview. In: MacGregor, D.S., Moody, R.T.J., Clark-Lowes, D.D. (Eds.), Petroleum Geology of
575 North Africa. Geological Society, London, Special Publication, 133, 217−229.

576 Guiraud, R., Bosworth, W., Thierry, J., Delplanque, A., 2005. Phanerozoic geological evolution of
577 Northern and Central Africa: an overview. Journal of African Earth Sciences, 43, 83–143.

578 Hansen, E., 1965. Methods of deducing slip line orientations from the geometry of folds. Carnegie
579 Institution of Washington Yearbook, 65, 387-405.

580 Hansen, E., 1967. Natural slip folds in which the fold axes nearly parallels the slip lines. Carnegie
581 Institution of Washington Yearbook, 66, 536–538.

582 Jaillard, E., Dumont, T., Ouali, J., Bouillin, J.P., Chihaoui, A., Latil, J.L., Arnaud, H., Arnaud-Vanneau, A.,
583 Zghal, I., 2013.The Albian tectonic “crisis” in Central Tunisia: nature and chronology of the
584 deformations. Journal of African Earth Sciences, 85, 75–86.

585 Jaillard, E., Bouillin, J. P., Ouali, J., Dumont, T., Latil, J. L., Chihaoui, A., 2013.Albian salt-tectonics in
586 Central Tunisia: Evidences for an Atlantic-type passive margin. Journal of African Earth Sciences, 135,
587 220−234.

588 Jaillard, E., Bouillin, J.P., Ouali, J., Dumont, T., Latil, J.L., Chihaoui, A., 2017.Albian salt tectonics in
589 Central Tunisia: evidences for an Atlantic-type passive margin. Journal of African Earth Sciences, 135,
590 220–234.

591 Jammeli, N., Souissi, F., Souissi, R., Guedria, A., Jrad, A., Naouali, H., 2011. Caractéristiques
592 pétrographiques, minéralogiques et géochimiques des affleurements triasiques et des
593 minéralisations de Jebel Ressass et ses environs (Tunisie nord orientale). Notes du Service
594 Géologique de Tunisie, 79 ,69-88.

595 Jones, O.T., 1939. The geology of the Colwyn Bay district: a study of submarine slumping during the
596 Salopian period. Quarterly Journal of the Geological Society of London, 380, 335-382.

597 Jones, O. T., 1940. On the sliding or slumping of submarine sediments in Denbighshire, North Wales,
598 during the Ludlow Period. Quarterly Journal of the Geological Society of London, 93, 241–283.

599 Kamoun, F., Peybernes, B., Ciszak, R., Calzada, S., 2001.Triassic paleogeography of
600 Tunisia.Palaeogeography, Palaeoclimatology, Palaeoecology, 172 (3-4) 223-242.

601 Khomsi, S., Roure, F., Khelil, M., Mezni, R., Echihi, O., 2019. A review of the crustal architecture and
602 related pre-salt oil/gas objectives of the eastern Maghreb Atlas and Tell: Need for deep seismic
603 reflection profiling. Tectonophysics, 766, 232–248.

604 Lamb, M. P., Myrow, P. M., Lukens, C., Houck, K., Strauss, J., 2008. Deposits from wave-Influenced
605 turbidity currents: Pennsylvanian Minturn formation, Colorado, U.S.A. Journal of sedimentary
606 research, 78, 480-498.

607 Marie, J., Trouvé, P., Desforges, G., Dufaure, P.H., 1982. Nouveaux éléments de paléogéographie du
608 Crétacé de Tunisie. Cretaceous Research, 3 (1), 167-170.

609 Martinez, C., Turki, M. M., Truillet, R., 1990. The signification of the meridian folds in the north-
610 central Tunisian Atlas. Bulletin de la societé géologique de France, 5, 843-852.

611 Martinez, C., Chikhaoui, M., Truillet, R., Ouali, J., Creuzot, G., 1991. Le contexte géodynamique de la
612 distension albo-aptienne en Tunisie septentrionale et centrale: structuration éocrétacée de l'Atlas
613 tunisien. EclogaegeologicaeHelvetiae, 84, 61–82.

614 Masrouhi, A., Ghanmi, M., Ben Slama, M.M., Ben Youssef, M., Vila, J.M., Zargouni, F., 2008. New
615 tectono-sedimentary evidence constraining the timing of the positive tectonic inversion and the
616 Eocene Atlasic phase in northern Tunisia: implication for the North African paleo-margin evolution.
617 ComptesRendus Geoscience,340, 771–778.

Masrouhi, A and Koyi, H. A., 2012.Submarine ‘salt glacier’ of Northern Tunisia, a case of Triassic salt mobility in North African Cretaceous passive margin. Geological Society, London, Special Publications, 363, 579-593.

Masrouhi, A., Bellier, O., Koyi, H., Vila, J.M., Ghanmi, M., 2013. The evolution of the Lansarine–Baouala salt canopy in the North African Cretaceous passive margin in Tunisia. Geological Magazine, 150 (5), 835–861.

Masrouhi, A., Bellier, O., Koyi, H., 2014b. Geometry and structural evolution of Lorbeus diapir, northwestern Tunisia: polyphase diapirism of the North African inverted passive margin. Int. J. Earth. Sci (GeolRundsch), 103, 881–900.

Masrouhi, A., Gharbi, M., Bellier, O., Ben Youssef, M., 2019. The Southern Atlas Front in Tunisia and its foreland basin: Structural style and regional-scale deformation. Tectonophysics, 764, 1-24.

Masse, J. P., & Borgomano, J., 1987. Un modèle de transition plate-forme-bassin carbonatés contrôlé par des phénomènes tectoniques: le Crétacé du Gargano (Italie Méridionale). Comptes rendus de l'Académie des sciences. Série 2, Mécanique, Physique, Chimie, Sciences de l'univers, Sciences de la Terre, 304(10), 521-526.

Mattoussi Kort, H., Gasquet, D., Ikenne, M., LaridhiOuazaa, N., 2009. Cretaceous crustal thinning in North Africa: implications for magmatic and thermal events in the Eastern Tunisian margin and the Pelagic Sea. Journal of AfricanEarth Sciences, 55 (5), 257–264.

Memmi L., 1981. Biostratigraphie du Crétacé inférieur de la Tunisie Nord-Orientale. Bull. Soc. Géol. France., (7), t XXIII, n°2, 157-183.

Memmi L., 1989. Le Crétacé inférieur (Berriasien-Aptien) de Tunisie. Biostratigraphie, Paléogéographie et Paléoenvironnements. Thèse Sci.Univ. Lyon I.157 p. inédite.

Morgan, M.A., Grocott, J., Moody, R.T.J., 1998. The Structural Evolution of the Zaghouan-Ressas Structural Belt, Northern Tunisia, 132. Geological Society London, Special Publications, pp. 405–422.

Naji, C., Gharbi, M., Amri, Z., Masrouhi, A., Bellier, O., 2018a. Temporal and spatial changes of the submarine Cretaceous paleoslope in Northern Tunisia, inferred from Slump folds analysis. Proceedings of the Geologists' Association, 129, 40–56.

Naji, C., Masrouhi, A., Amri, Z., Gharbi, M., Bellier, O., 2018b. Cretaceous paleomargin tilted blocks geometry in northern Tunisia: stratigraphic consideration and fault kinematic analysis. Arabian Journal of Geosciences, 11:583.

Ouahchi, A., Bismuth, H., Turki, M. M., 1993. Nouvelles données sur le Crétacé et l'Eocène des environs deGrombalia (Tunisie nord-orientale). Géologie Méditerranéenne, 20, 1, 25-43.

Piqué, A., Tricart, P., Guiraud, R., Laville, E., Bouaziz, S., Amrhar, M., Ait Ouali, R., 2002.The Mesozoic–Cenozoic Atlas belt (North Africa): an overview. GeodinamicaActa, Volume 15, Issue 3, 185-208.

Ritz, J.F., Taboada, A., 1993. Revolution stress ellipsoids in brittle tectonics resulting from an uncritical use of inverse methods. Bull. Soc. Geol. Fr. 164 (4), 519–531.

Rosenbaum, G., Lister, G.S., Duboz, C., 2002. Relative motions of Africa, Iberia and Europe during Alpine orogeny. Tectonophysics 359, 117–129.

Saadi. J., 1990. Exemple de sédimentation syntectonique au Crétacé inférieur le long d'une zone de décrochement NS. Les structures d'Enfidha (Tunisie nord-orientale). Géodynamique, 5, 1, 17-33.

Santantonio, M., Scrocca, D., Lipparini, L., 2013. The Ombrina-Rospo Plateau (Apulian Platform): Evolution of a carbonate platform and its margins during the Jurassic and Cretaceous. Marine and Petroleum Geology, 42, 4-29.

Sebei, K., Amiri, A., Abidi, O., Manai, D., Inoubli, M. H., Salem, A. B., 2019. Episodes with reefal formations during the Aptian–Late Cretaceous in the gulf of Hammamet (Northeastern Tunisia): insights from seismic reflection and wells data. International Journal of Earth Sciences, 108(3), 779-797.

Sharman, G.R., Graham, S.A., Masalimova, L.U., Shumaker, L.E., King, P.R., 2015. Spatial patterns of deformation and paleoslope estimation within the marginal and central portion of a basin-floor mass-transport deposit, Taranaki Basin, New Zealand. Geosphere, 11, 266-306.

Slama, M.-M.B., Masrouhi, A., Ghanmi, M., Youssef, M.B., Zargouni, F., 2009. Albian extrusion evidences of the Triassic salt and clues of the beginning of the Eocene atlasic phase from the example of the Chitana-Ed Djebs structure (N.Tunisia): Implication in the North African Tethyan margin recorded events, comparisons. Comptes Rendus - Geoscience, 341, 7, 547-556.

Snoke, A. W., Schamel, S., Karasek, R. M., 1988. Structural evolution of DjebelDebadib anticline: A clue to the regional tectonic style of the Tunisian Atlas. Tectonics, 7 (3), 497-516.

Soua, M., Echihi, O., Herkat, M., Zaghbib-Turki, D., Smaoui, J., Fakhfakh-Ben Jemia, H., Belghaji, H., 2009.Structural context of the paleogeography of the Cenomanian- Turonian anoxic event in the eastern Atlas basins of the Maghreb. Cretaceous Research, 341, 1029-1037.

677 Soua, M., 2016. Cretaceous oceanic anoxic events (OAEs) recorded in the northern margin of Africa
678 as possible oil and gas shale potential in Tunisia: an overview. International Geology Review, 58 (3),
679 277–320.

680 Souquet, P., Peybernes, B., Saadi, J., Ben Youssef, M., Ghanmi, M., Zarbout, M., Chikhaoui, M.,
681 Kamoun, F., 1997.Séquences et cycles d'ordre 2 en régime extensif et transtensif: exemple du
682 Crétacé inférieur de l'Atlas tunisien. Bulletin de la Société géologique de France, 168, 373–386.

683 Soussi, M., Mangold, C., Enay, R., Boughdiri, M., Ben Ismail, M.H., 2000.The Lower and Middle
684 Jurassic of Northern Tunisia; correlations with the North-South axis and palaeogeography. Geobios,
685 33, 4, 437–446.

686 Soussi, M., 2003.New Jurassic lithostratigraphic chart for the Tunisian atlas.Geobios, 36, 761–773.

687 Soussi, M., Niedźwiedzki, G., Tałanda, M., Dróżdż, D., Sulej, T., Boukhalfa, K., Mermer, J., Błażejowski,
688 B., 2017. Middle Triassic (Anisian-Ladinian) Tejra red beds and Late Triassic (Carnian) carbonate
689 sedimentary records of southern Tunisia Saharan Platform: biostratigraphy, sedimentology and
690 implication on regional stratigraphic correlations. Marine and Petroleum Geology, 79, 222–256.

691 Sperner, B., Ratschbacher, L.R., 1993. Fault-striae analysis: a TURBO PASCAL program package for
692 graphical presentation and reduced stress tensor calculation. Computer Geosciences, 19, 1361–1388.

693 Stampfli, G. M., Borel, G. D., Marchant, R., Mosar, J., 2002. Western Alps geological constraints on
694 western Tethyan reconstructions. In: Rosenbaum, G. and Lister, G. S. 2002. Reconstruction of the
695 evolution of the Alpine-Himalayan Orogen. Journal of the Virtual Explorer, 7, 75–104.

696 Stampfli, G. M. and Hochard, C., 2009. Plate tectonics of the Alpine realm.Geological Society London
697 Special Publications.

698 Strachan, L. J., Alsop, G. I., 2006. Slump folds as estimators of palaeoslope: a case study from the
699 Fisherstreet Slump of County Clare, Ireland. Basin Research, 18, 451–470.

700 Strachan, L. J., 2008. Flow transformations in slumps: a case study from the Waitemata Basin, New
701 Zealand. Sedimentology, 55, 1311−1332.

702 Tavani, S., Vignaroli, G., Parente, M., 2015. Transverse versus longitudinal extension in the
703 foredeep-peripheral bulge system: Role of Cretaceous structural inheritances during early Miocene
704 extensional faulting in inner central Apennines belt. Tectonics, 34 (7), 1412-1430.

Tlig, S., 2015. The upper jurassic and lower cretaceous series of southern Tunisia and northwestern Libya revisited. Journal of African Earth Sciences, 110, 100–115.

Tranos, M.D., 2017. The use of Stress Tensor Discriminator Faults in separating heterogeneous fault-slip data with best-fit stress inversion methods. Journal of structural geology, 102, 168–178.

Turki, M. M., 1985. Polycinématique et contrôle sédimentaire associée sur la cicatrice Zaghouan-Nebhana. Thèse Doctorat d'Etat, Université de Tunis et Revue Sciences de la Terre, C.S.T-I.N.R.S.T, 7, 228 pp.

Turki, M.M., 1988. Les inversions tectoniques de la Tunisie centro-septentrionale. Bulletin de la Société Géologique de France, 8 (3), 399–406.

Vila, J. M., Ben Youssef, M., Bouhlel, S., Ghanmi, M., Kassâa, S., Miaadi, F., 1998. Tectonique en radeaux au toit d'un ''glacier de sel'' sous-marin albien de Tunisie du Nord-Ouest: exemple du secteur minier de GueurnHalfaya. Comptes Rendus de l'Académie des Sciences, 327, 563-570.

Woodcock, N.H., 1976a.Ludlow Series slumps and turbidites and the form of the Montgomery Trough, Powys, Wales. Proceedings of the Geologists Association, 87, 169–182.

Woodcock, N.H., 1976b. Structural style in slump sheets: Ludlow series Powys, Wales. Journal of the Geological Society, London, 132, 399–415.

Woodcock, N. H., 1979. The use of slump structures as palaeoslope orientation estimators. Sedimentology, 26, 83−99.

Yong, L. I., Zhufu, S., Cui, M., Yuping, Y., Shengxin, L., 2013. The seismic induced soft sediment deformation structures in the Middle Jurassic of Western Qaidamu Basin. Acta Geologica Sinica, 87, 4, 979−988.

Figures captions

Figure 1: Geological map of the study area (Slightly modified from Turki, 1985). The inset in the top right shows the location of the study area in northeastern Tunisia.

Figure 2: Fold patterns in slump trigger. A) Model used to relate slump fold geometry to paleoslope attitude (Slightly modified from Woodcock, 1976b). B) Equal area plot of hypothetical fold axis and poles of axial planes disposition to explain the mean axis, the separation, and the axial plane methods. The best fit girdle to axes and poles to axial planes of the slump sheet are rotated to their horizontals. The inferred paleoslope plunges to south (modified from Woodcock, 1979). C) folding inducing during layer-parallel shearing (a) and layer-normal shearing (b), see Alsop and Marco,2011 for more detail, and, associated facing direction (for more detail see Alsop and Marco,2011, 2012a). D) Fold facing orientation in schematic simulations summarizing the relationships between slump folds vergence, axial plane and up-ward or downward facing states (see Alsop and Marco, 2012a).

Figure 3: Lithostratigraphic correlation of Cretaceous series of Bou Kournine-Borj Cedria with surrounding area (Jebel Mekki and Jebel El Khourija). The inset in the Midst shows the location of measured sections in northeastern Tunisia.

Figure 4: Photographic plate illustrating significant tectono-sedimentary features in the study area. A) Panoramic view looking to the north showing the outcropping Barremian-Turonian series. B) Field photo showing abundant meso-scale normal faults, sometimes with horst and graben geometry in the Barremian strata of Borj Cedria area. C) Small-scale normal fault preserved in the sandy limestone Barremian strata of the same area. D) Field photo showing small-scale extensive deformation preserved showing a sealed normal fault in the Aptian sequences of Bou Kournine-Borj Cedria area. E) Small-scale normal fault preserved in the nodular Cenomanian limestone series of Jebel Srara (Borj Cedria area). F) Field photo showing abundant small-scale normal faults drawing horst and graben geometry in the nodular Cenomanian limestone strata of the same area.

Figure 5: Simplified geologic map (extracted from Fig. 1) with the back-tilted stress tensors of Barremian, Aptian and Cenomanian-Turonian fault populations collected from the study area with the use of the Win-Tensor program (Delvaux, 2016). Fault slip data are computed throughRight Dihedron method.

Figure 6: Lower hemisphere projection of back-tilted major fault data sets showing the regional paleostress regime in the study area during Barremian and Albian times.

Figure 7: Structural data from slump folds with inferred paleoslope direction during Barremian in Bou Kournine-Borj Cedria area. A, B, C, D, E, F) Field photos that show well-preserved Barremian slump folds. G) Equal area projection of restored (back-tilted) slump axis (blue box) and poles to axial planes (red box) with respectively MAM (blue arrow) and APM (red arrow) methods.

Figure 8: Structural data from slump folds with inferred paleoslope direction during Albian in Borj Cedria-Bou Kournine area. A, B, C, D, E, F) Field photos that show well preserved decametric Albian slump folds. G) Equal area projection of unfolded slump axis (blue box) and poles to axial planes (red box) with respectively MAM (blue arrow) and APM (red arrow) methods.

Figure 9: Paleocurrent orientation from the study area inferred from directional syn-sedimentary structures with: a) Hummocky cross stratifications (HCS) with flute casts (F) collected from Barremian strata. b, c, d) Flute casts (F) and groove marks (G) collected from Hauterivian-Barremian strata. e) Reworked blocks (R) in the Barremian deposits. F) Rose diagram illustrating the paleocurrent direction inferred from different directional sedimentary data sets (Flute casts, groove marks. etc…).

Figure 10: Simplified present-day structural configuration of Borj Cedria-Bou Kournine area: A, B, C) Paleogeographic reconstruction map of the western Tethyan domain during respectively Bathonian, Hauterivian and Albian times (From Stampfli and Hochard, 2009) with inferred paleoslope assessment (colored arrow). The blue rectangle indicates the paleogeographic position of Tunisia. D) Simplified cross-section across Borj Cedria-Bou Kournine area (slightly modified from Turki et al., 1988) showing the present-day structural configuration of this area together with the related deposits (lithostratigraphic sections). The inset in the left shows the location of the study area in northeastern Tunisia.

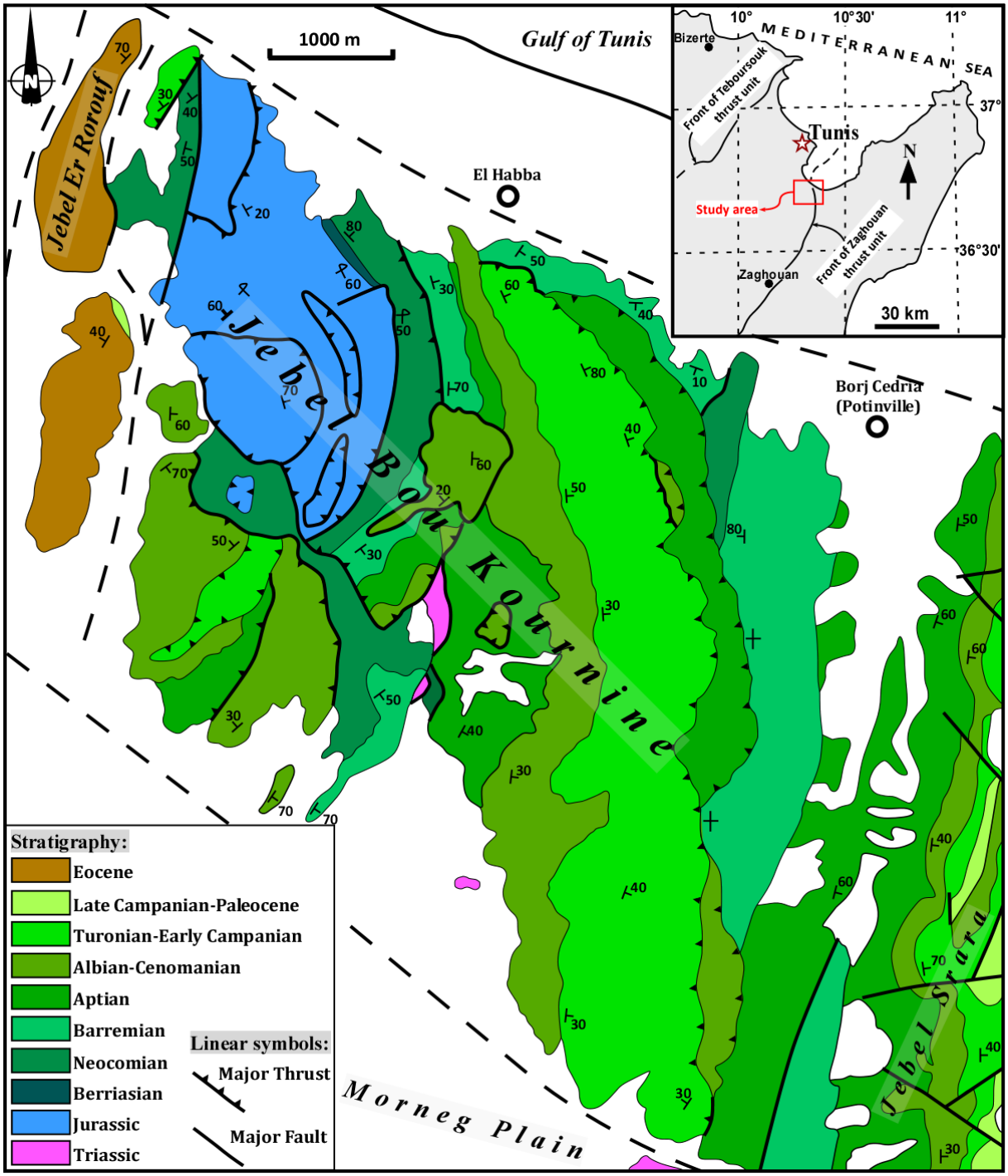

792

793 **Figure 1**

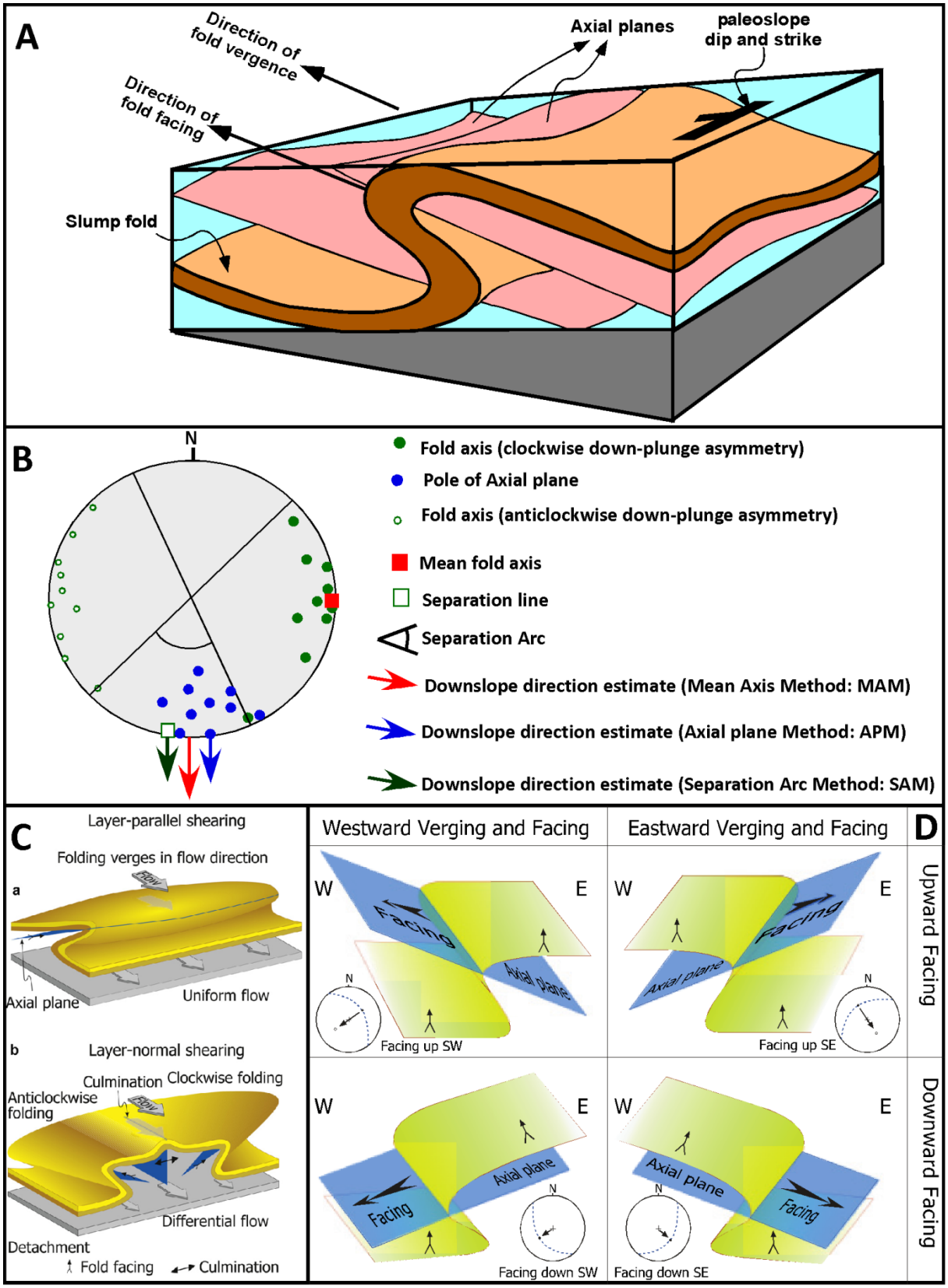

794

795 **Figure 2**

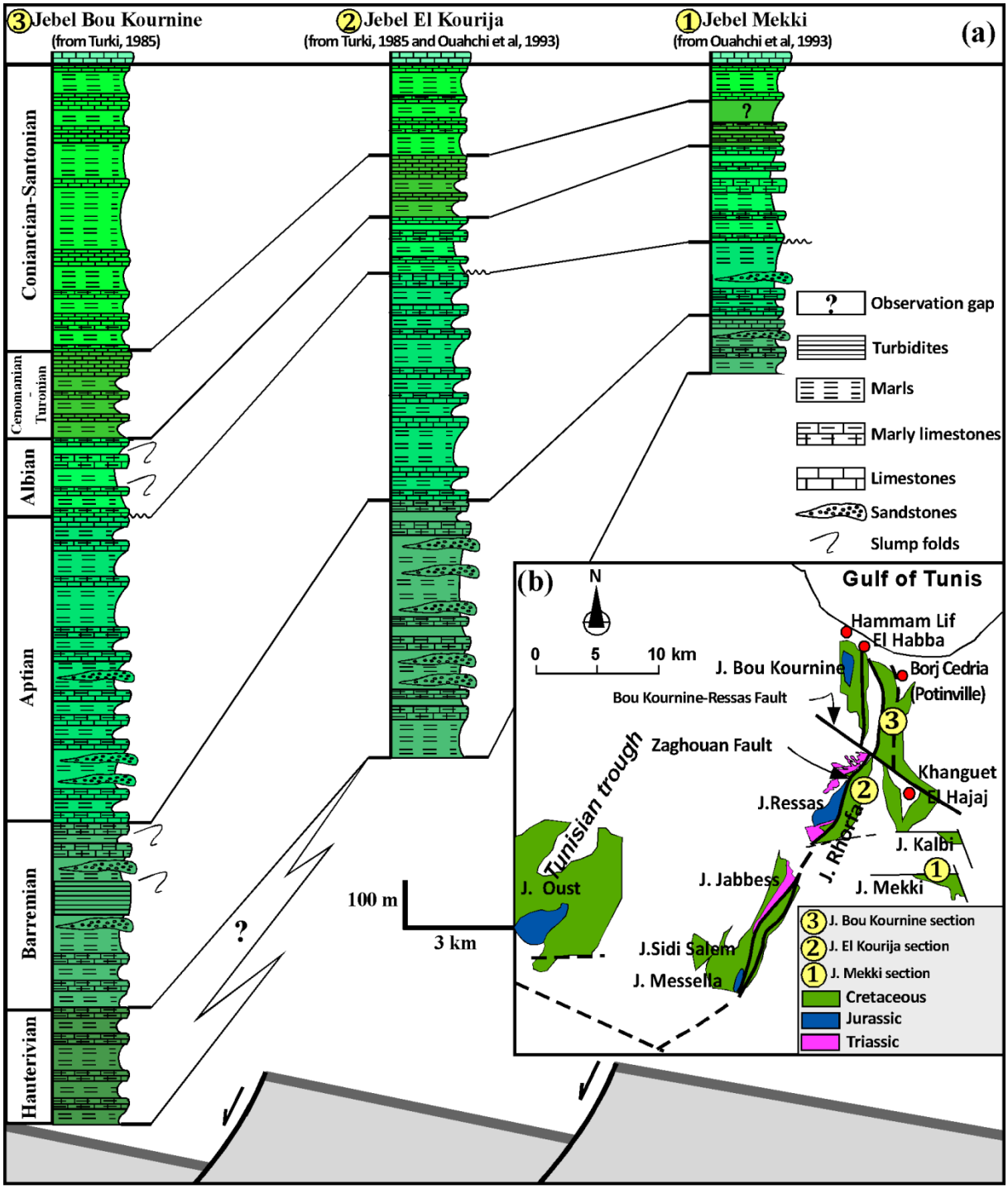
3 Jebel Bou Kournine
(from Turki, 1985)
2 Jebel El Kourija
(from Turki, 1985 and Ouahchi et al, 1993)
1 Jebel Mekki
(from Ouahchi et al, 1993)
(a)
Coniancian-Santonian
Cenomanian
Turonian
Albian
Aptian
Barremian
Hauterivian
?
Observation gap
Turbidites
Marls
Marly limestones
Limestones
Sandstones
Slump folds
100 m
3 km
(b)
N
0 5 10 km
Gulf of Tunis
Hammam Lif
El Habba
J. Bou Kournine
Borj Cedria
(Potinville)
Bou Kournine-Ressas Fault
Zaghouan Fault
Tunisian trough
Khanguet
El Hajaj
J.Ressas
J. Rhorfa
J. Kalbi
J. Oust
J. Jabbess
J. Mekki
J.Sidi Salem
J. Messella
3 J. Bou Kournine section
2 J. El Kourija section
1 J. Mekki section
Cretaceous
Jurassic
Triassic

Figure 3

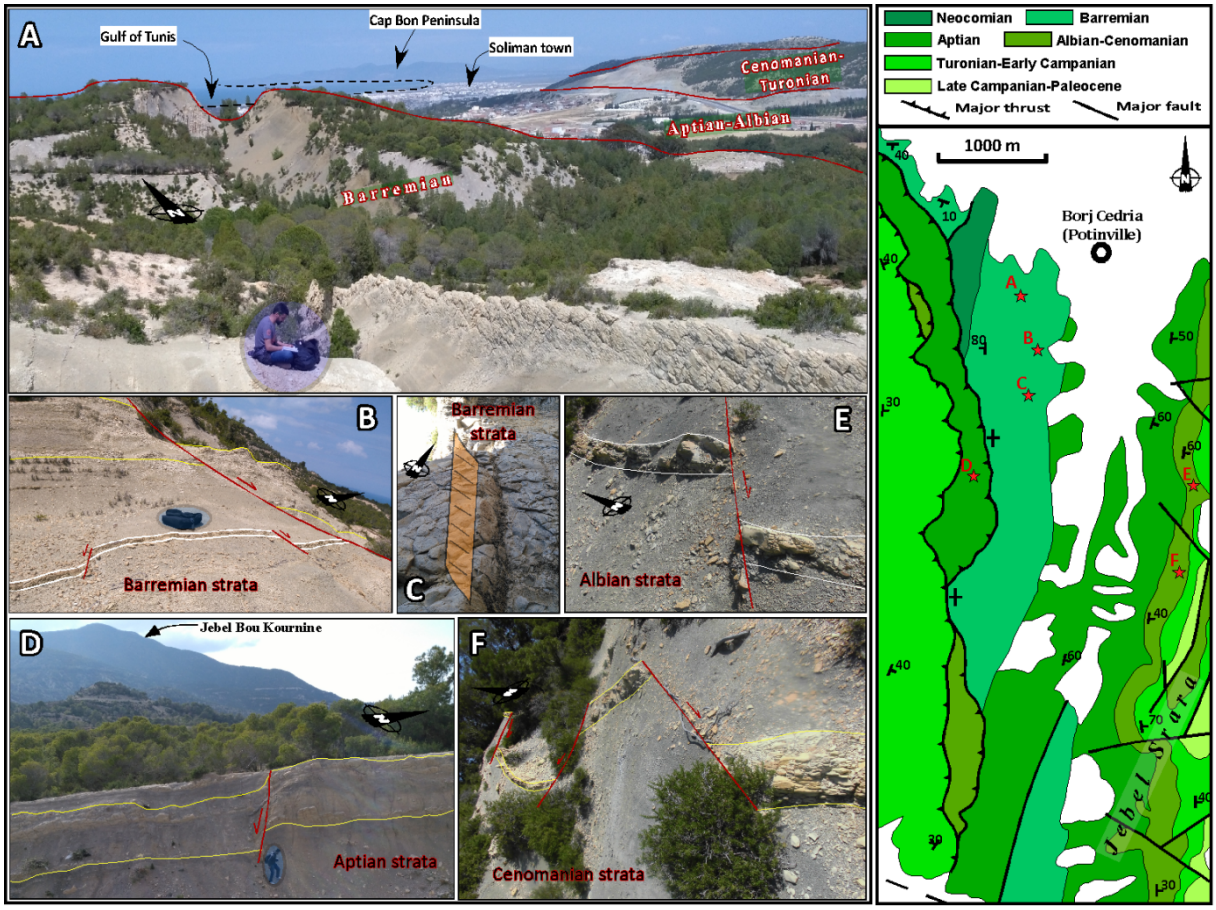

798

799 **Figure 4**

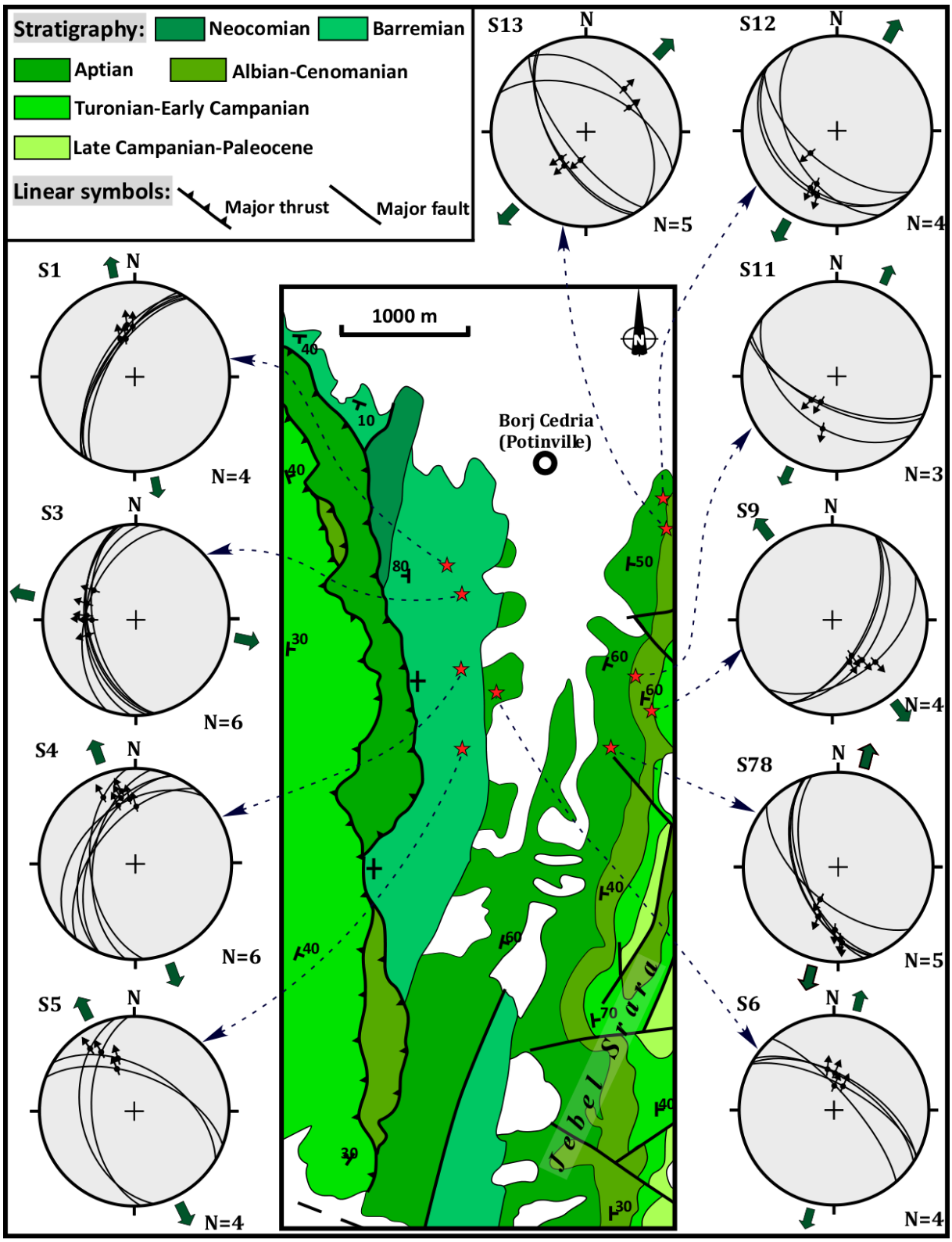

800

801 **Figure 5**

802

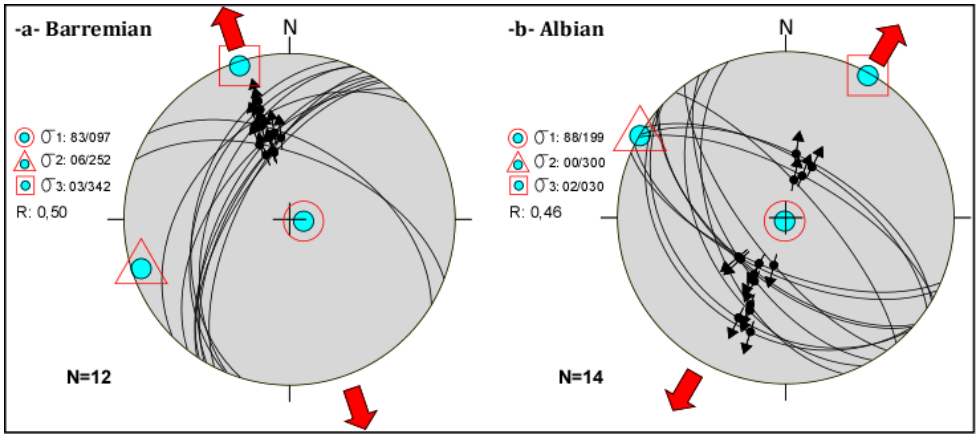

803 **Figure 6**

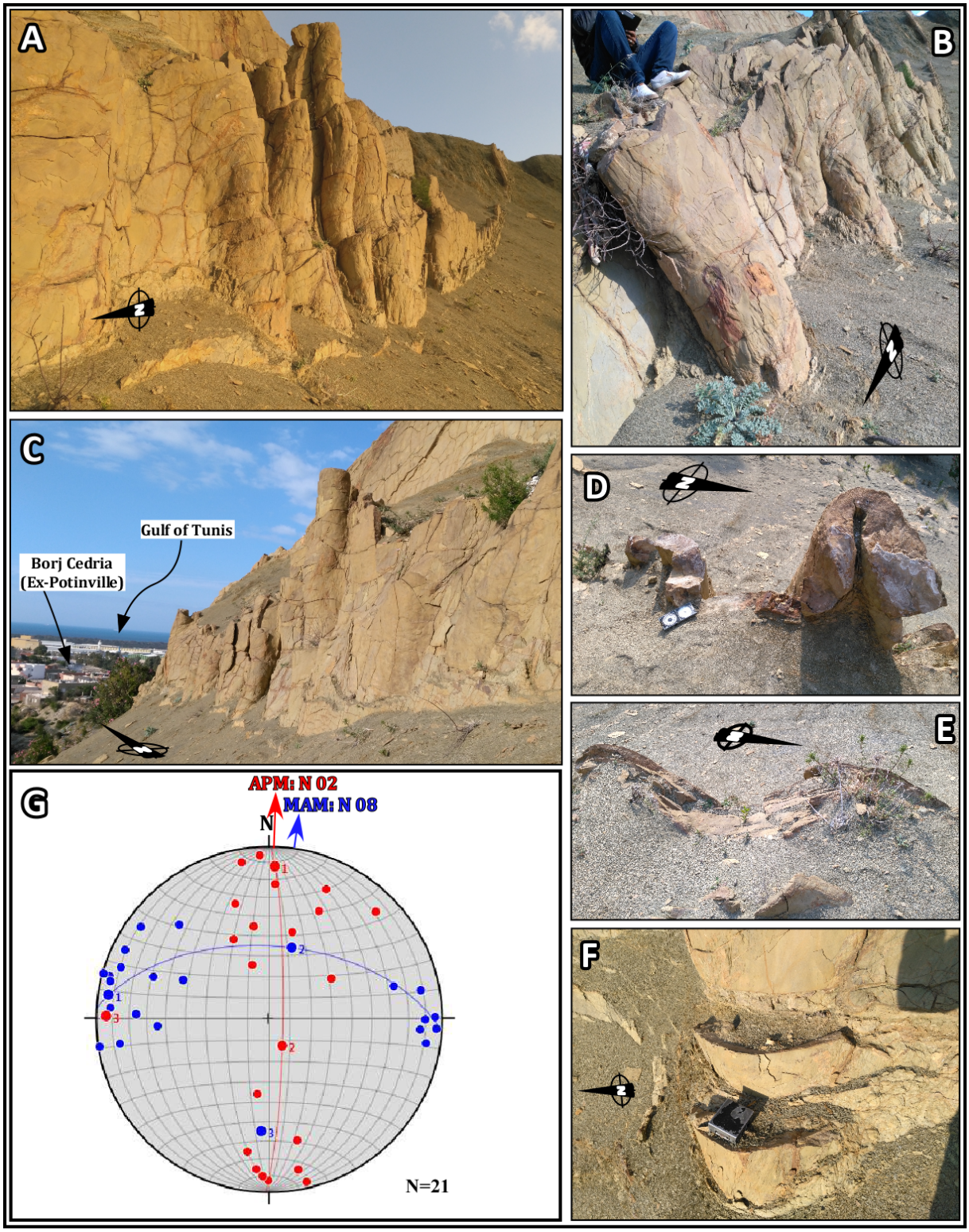

804

805 **Figure 7**

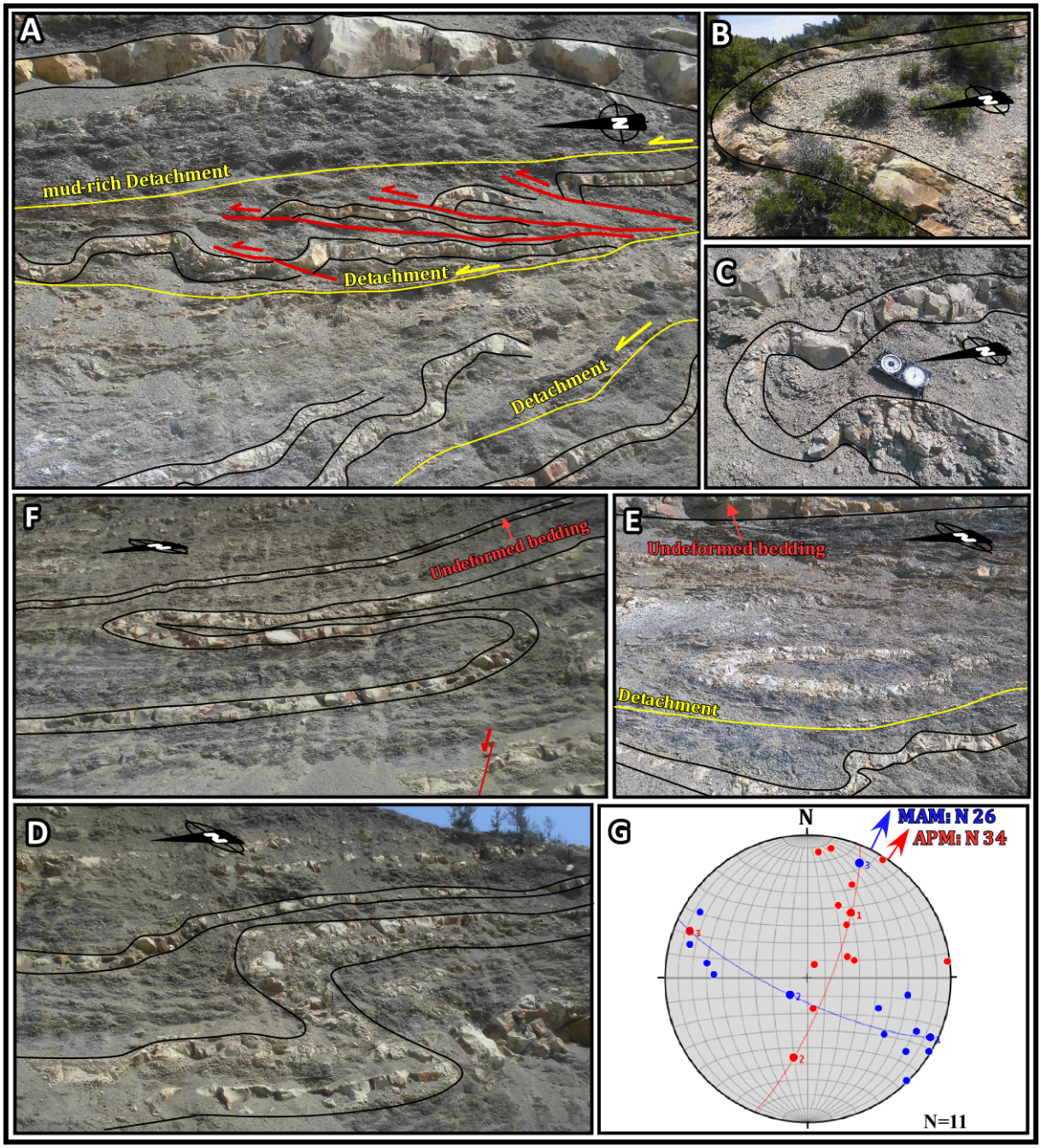
A
mud-rich Detachment
Detachment
Detachment
B
C
F
Undeformed bedding
E
Undeformed bedding
Detachment
D
G
N
MAM: N 26
APM: N 34
N=11

Figure 8

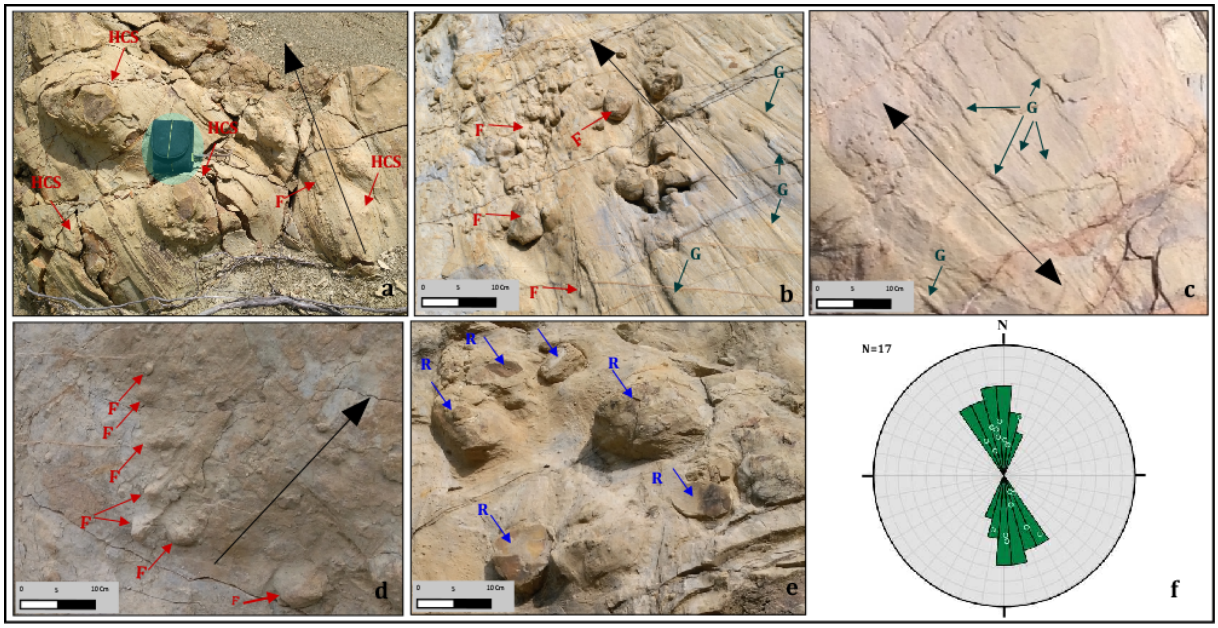

808

809 **Figure 9**

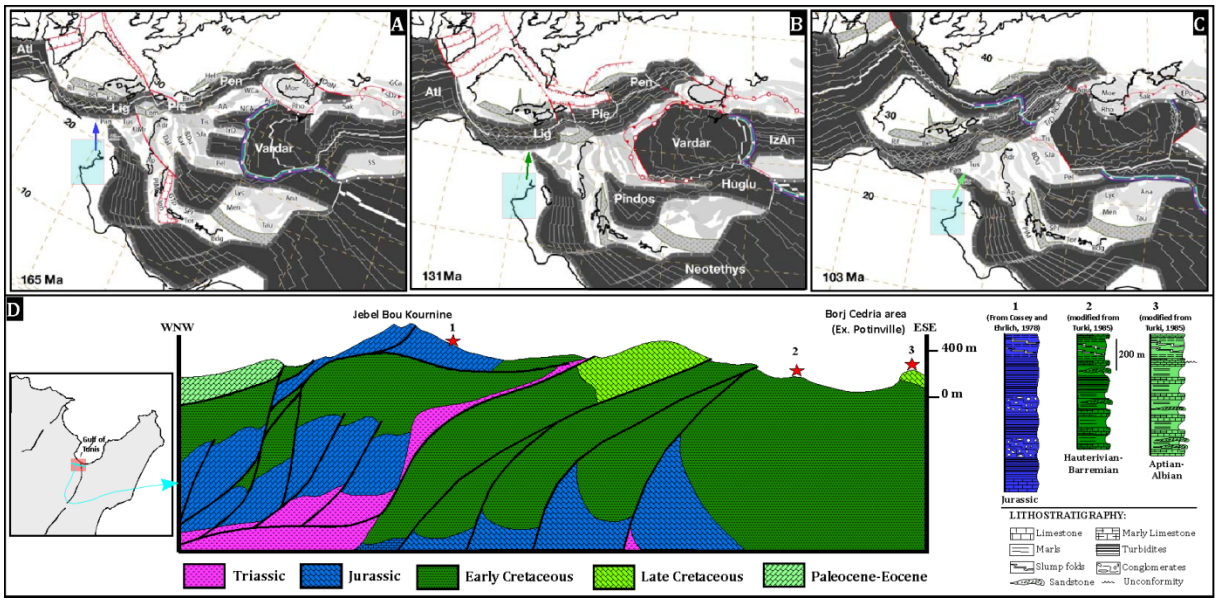

810

811 **Figure 10**